# A New Chalcone Derivative (*E*)-3-(4-Methoxyphenyl)-2-methyl-1-(3,4,5-trimethoxyphenyl)prop-2-en-1-one Suppresses Prostate Cancer Involving p53-mediated Cell Cycle Arrests and Apoptosis

YONG ZHANG[1,3], BALASUBRAMANIAN SRINIVASAN[2], CHENGGUO XING[2] and JUNXUAN LÜ[1,3]

[1]*Hormel Institute, University of Minnesota, Austin, MN, U.S.A.;*
[2]*Department of Medicinal Chemistry, University of Minnesota College of Pharmacy, Minneapolis, MN, U.SA.;*
[3]*Department of Biomedical Sciences, TTUHSC School of Pharmacy, Amarillo, TX, U.S.A.*

**Abstract.** *Previous studies suggested chalcones as antineoplastic drug candidates. We synthesized a new chalcone derivative (E)-3-(4-methoxyphenyl)-2-methyl-1-(3,4,5-trimethoxyphenyl)prop-2-en-1-one, (CHO27) with an up to 1000-fold increased cytotoxic potency relative to its parent compound in cell culture assays. CHO27 at low nanomolar levels, inhibited prostate cancer (PCa) cell growth through cell cycle arrest and caspase-dependent apoptosis. Activation of p53 accounted for, at least in part, the growth inhibition by CHO27 in vitro. Furthermore, i.p. administration of CHO27 suppressed the growth of established PCa 22Rv1 xenograft tumors accompanied with p53 and p21^{Cip1} induction. CHO27 may be a lead for development of new therapeutic agents for PCa.*

Prostate cancer (PCa) is responsible for estimated 30,000 deaths per year and is the second leading cause of cancer-related death in American men (1). Current therapies for advanced-stage PCa by hormone ablation cause transitory remission of the disease. However, the malignancy will invariably relapse to aggressive castration-resistant prostate cancer (CRPCa). As a first-line chemotherapy drug approved by the FDA for CRPCa, docetaxel, along with prednisone, provides only a 2-month survival benefit for patients (2). The

*Correspondence to:* Junxuan Lü, Hormel Institute, University of Minnesota, 801 16th Avenue NE, Austin, MN 55912, U.S.A. E-mail: Junxuan.lu@ttuhsc.edu and Chengguo Xing, Department of Medicinal Chemistry, University of Minnesota College of Pharmacy, 8-101 Weaver-Densford Hall, 308 Harvard Street SE, Minneapolis, MN 55455, U.S.A. E-mail: Xingx009@umn.edu

*Key Words:* Chalcone derivative, prostate cancer cells, p53, cell cycle arrest, apoptosis.
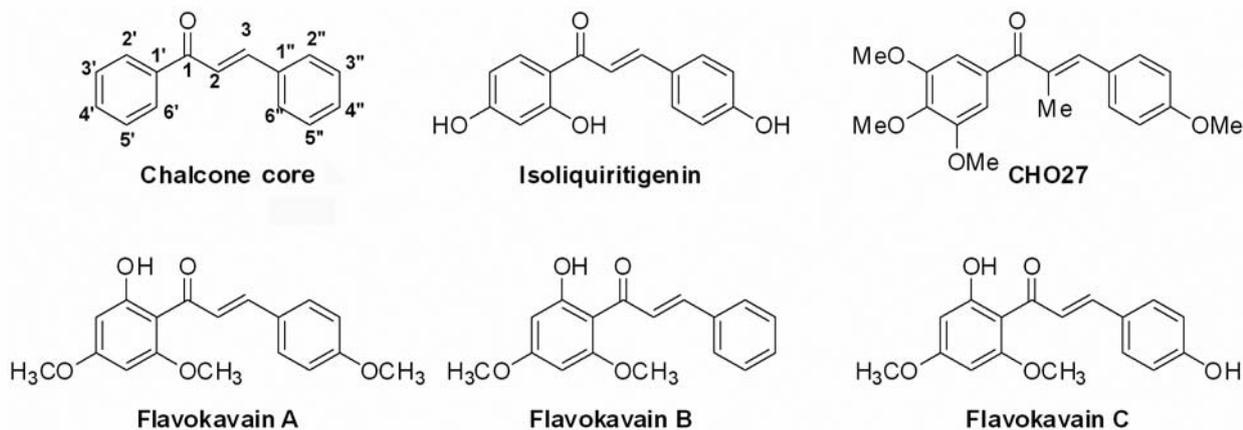
newly approved drugs in the last two years (androgen synthesis blocker abiraterone acetate and novel taxane cabarzitaxel) for docetaxel-resistant CRPCa add a further survival of 2-3 months (3, 4). The development of new therapeutic agents is surely needed.

Chalcones are a class of compounds containing a central 1,3-diphenyl-prop-2-en-1-one structure known as "chalcone core" (Figure 1), which consists of two aromatic rings jointed by the three-carbon $\alpha$, $\beta$-unsaturated carbonyl system (5). Recent studies, including our own, have shown that chalcones possess potential inhibitory activities against various cancer cells including prostate (6-8), kidney (9, 10), colon (11-13), lung (14-17), breast (16, 18), liver (10, 19, 20), bladder (21, 22), leukemia (23) and skin cancers (24), through induction of apoptosis and cell cycle arrest (25, 26). Mechanically, the tumor suppressor p53 has been identified as a molecular target associated with the inhibitory actions of some chalcones (13, 18, 27-29). Several reports suggest that some chalcones exhibit an inhibitory preference for p53-wild type cancer cells than p53-mutant or -null cancer cells (13, 27-29), and their inhibitory activities depended on a functional activation of p53 (28, 29). Most of these p53-selective chalcones, however, exerted modest *in vitro* anticancer activity with no significant *in vivo* activity, prompting the development of more potent chalcone derivatives for further evaluation.

In the present study, we synthesized a new chalcone derivative CHO27, (*E*)-3-(4-methoxyphenyl)-2-methyl-1-(3,4,5-trimethoxyphenyl)prop-2-en-1-one (Figure 1) with greater potency against various cancer cells than the parent compound and other chalcone-based natural products. In prostate cancer models, CHO27 exhibited a strong suppression of cell growth *in vitro* in association with p53-induced cell cycle arrests and apoptosis. *In vivo* administration of CHO27 in a therapy context suppressed the growth of established aggressive 22Rv1 PCa xenografts.

Figure 1. *Structures and numbering of chalcone core, chalcone-based natural products and CHO27. Chalcone core: 1, 3-diphenyl-prop-2-en-1-one; Isoliquiritigenin, flavokavain A, B and C: chalcone-based natural products; CHO27: (E)-3-(4-methoxyphenyl)-2-methyl-1-(3,4,5-trimethoxyphenyl)prop-2-en-1-one.*

## Materials and Methods

*Synthesis and characterization.* (E)-3-(4-Methoxyphenyl)-2-methyl-1-(3,4,5-trimethoxyphenyl)prop-2-en-1-one: 1-(3,4,5-trimethoxyphenyl) propan-1-one was prepared from 3,4,5-trimethoxybenzaldehyde. Grignard reaction of ethylmagnesium chloride on 3,4,5-trimethoxybenzaldehyde followed by pyridinium chlorochromate oxidation of the resulting secondary alcohol afforded 1-(3,4,5-trimethoxyphenyl)propan-1-one. To a mixture of 1-(3,4,5-trimethoxyphenyl)propan-1-one (2.24g, 0.01 mol) and 4-methoxybenzaldehyde (1.36g, 0.01 mol equiv) in anhydrous MeOH (30 mL), NaOH (1.2g, 0.003 mol) was added and stirred at room temperature for 24 h. The reaction mixture was acidified to pH 5 using aqueous hydrochloric acid (10%) followed by extraction with ethyl acetate (3×50 ml). The combined organic layer was dried over anhydrous sodium sulfate and concentrated under reduced pressure to afford crude product. The crude product thus obtained was purified by silica gel column chromatography using ethyl acetate: hexane; 1:3 to produce (E)-3-(4-methoxyphenyl)-2-methyl-1-(3,4,5-trimethoxyphenyl)prop-2-en-1-one in 86% yield. $^1$H NMR (400MHz, CDCl$_3$): δ 7.35 (2H, d, *J*=7.8 Hz), 7.1 (1H, s), 6.94 (2H, s), 6.88 (2H, d, *J*=8.0 Hz), 3.85 (3H, s), 3.81 (6H, s), 3.77 (3H, s), 2.21 (3H, s). $^{13}$C NMR (100 MHz, CDCl$_3$): δ. 198.5, 153.1, 147.2, 144.6, 141.2, 135.0, 133.5, 129.0, 128.5, 110.5, 107.2, 60.8, 56.2, 55.0, 14.8, MS (ESI, positive) m/z calculated for C$_{20}$H$_{22}$O$_5$ (M+H): 343.15; found 343.2. Other chalcone-based natural products were prepared following our previous reported methods (14).

*Cell culture.* Human PCa cells (LNCaP, 22Rv1, DU 145 and PC-3), lung cancer cells (NCI-H460), colon cancer cells (HCT 116) and pancreatic cancer cells (SU.86.86) were obtained from the American Type Culture Collection (ATCC, Manassas, VA). C4-2 cells (a castration-resistant derivative of LNCaP) were kindly provided by Dr. Donald Tindall (Mayo Clinic, Rochester, MN, USA). Among these cells, LNCaP, C4-2, NCI-H460 and HCT 116 cells harbor wild-type p53 (referred as p53-wt), 22Rv1 cells harbor a mutant p53 which does not negatively affect the function of p53 (referred as p53-functional). DU 145 and SU.86.86 cells harbor mutant p53 which inactivates the function of p53 (referred as p53-mutant), and PC-3 cells are null for p53. Dominant-negative (DN) mutant p53

LNCaP-DN-P151S and the vector-transfected cells were generously provided by Dr. Ralph W. deVere White (Department of Urology, University of California, Davis, CA, USA). HCT 116-p53$^{+/+}$ and isogenic HCT 116-p53$^{-/-}$ cells developed in Dr. Bert Vogelstein's lab (HCT 116 cells with wild-type p53 or deleted p53, respectively) were kindly provided by Dr. Yibin Deng (University of Minnesota Hormel Institute, Austin, MN). All cells were cultured in the standard 37°C and 5% CO$_2$ humidified environment.

*Cytotoxicity screening.* The cytotoxicity screening of the chalcone candidates against four human cancer cell lines followed a previously published procedure (14). In brief, cells were plated in a 96-well plate and exposed to indicated compounds with a series of 3-fold dilution for 48 h, then the relative cell viability in each well was determined by using the CellTiter-Blue Cell Viability Assay Kit (Promega, San Luis Obispo, CA).

*Growth inhibition assay.* Based on its much increased cytotoxicity potency profile, CHO27 was chosen for further evaluation with additional PCa cell lines. Crystal violet staining of cellular proteins was used to evaluate the growth inhibition of PCa cells exposed to CHO27, as previously described (30). Briefly, PCa cells were exposed to indicated treatments, and then the cells that remained attached were stained with 0.02% crystal violet. After thorough rinsing with water, the cell-retained crystal violet was dissolved in 70% alcohol for photometric reading to estimate the cell number.

*Cell cycle distribution and BrdU incorporation rate.* PCa cells were exposed to indicated concentrations of CHO27 for 24 h, and then bromodeoxyuridine (BrdU) was added to the medium (1 μM of final concentration) for another 30 min. The cells were collected by trypsinization for cell cycle distribution and BrdU incorporation flow cytometric measurement, as previously described (31).

*Immunoblotting.* The whole cell lysate was prepared for immunoblotting detection of proteins of interest as previously described (32). The antibodies against cleaved poly (ADP-ribose) polymerase (PARP) and phospho-p53 (ser15) were obtained from Cell Signaling Technology (Beverly, MA, USA). The antibodies

Table I. *Growth inhibitory potency screening of the plain chalcone, chalcone-based natural products and CHO27 against four human cancer cells.*

| | DU145 | HCT116 | NCI-H460 | SU.86.86 |
|---|---|---|---|---|
| | $IC_{50}$ (μM) | | | |
| Chalcone | 17.4±2.7 | 5.48±0.69 | 11.2±1.8 | 5.25±0.72 |
| Isoliquiritigenin | 18.6±3.5 | 16.0±1.1 | 15.2±2.6 | 27.3±5.1 |
| Flavokavain A | 14.1±1.4 | 18.9±1.5 | 8.05±1.56 | 17.7±2.8 |
| Flavokavain B | 8.20±1.20 | 6.58±0.83 | 5.78±1.01 | 7.12±1.19 |
| Flavokavain C | 15.1±2.5 | 12.9±1.5 | 9.18±1.59 | 12.3±2.1 |
| CHO27 | 0.037±0.003 | 0.0064±0.0011 | 0.011±0.001 | 0.030±0.003 |

$IC_{50}$: Half maximal inhibitory concentration. The experiments were run in triplicate. Each value represents mean±SEM.

against p53 and p21[Cip1] were obtained from Leica Microsystems Inc. (Buffalo Grove, IL, USA) and EMD Chemicals Inc. (Philadelphia, PA, USA), respectively.

*Apoptosis evaluation.* After exposure to CHO27 and/or a general caspase inhibitor zVADfmk (R&D system, Minneapolis, MN, USA) for 72 h, the cells were collected for apoptosis evaluation by a number of methods. The first was Death ELISA detection of apoptotic DNA nucleosomal fragmentation, after gently lysing the cells and releasing histone-associated nucleosomal fragmentation using the Cell Death ELISA System Double Sandwich Kit (Roche Diagnostics GmbH, Mannheim, Germany), according to the users' manual (33). The second was Annexin V staining of externalized phosphatidylserine in apoptotic cells by flow cytometry using the Annexin V-FITC Detection Kit (MBL International, Inc., Watertown, MA, USA) following the users' manual (34). The third method was immunoblotting detection of cleaved PARP, as described previously (35).

*Measurement of CHO27 in mouse plasma.* The animal studies were approved by the Institutional Animal Care and Use Committee (IACUC) of University of Minnesota, and were carried out at the Hormel Institute animal facility. Fifteen male C57BL/6J mice were randomly assigned into five groups (n=3 per group), and received vehicle (dimethyl sulfoxide [DMSO]: ethanol: polyethylene glycol 400 [PEG 400]: Tween 80: 5% glucose=1.5: 1.5: 6: 1: 20) or CHO27 (1 mg per mouse, ~40 mg/kg) *via* intraperitoneal (*i.p.*) injection, respectively. At the indicated time points, the mice were anesthetized for blood collection and plasma preparation. CHO27 was extracted from the plasma and analyzed using a high performance liquid chromatography (HPLC) system as previously described (36).

*In vivo efficacy of CHO27 against PCa 22Rv1 xenograft tumors.* Male Nu/Nu nude mice were purchased from the Charles River Labs (Wilmington, MA). At 6 weeks of age, the mice were subcutaneously inoculated with $2×10^6$ aggressive castration-resistant 22Rv1 cells on the right flank. When the xenograft tumors grew to approximately 400 mm³, the mice were randomly assigned into two groups (n=11, respectively) and were given, once daily, treatment with vehicle (DMSO: ethonal: PEG400: Tween 80: 5% glucose=1.5: 1.5: 6: 1: 20) or CHO27 (1 mg per mouse, ~40 mg/kg) *via i.p.* injection, respectively. The mice were monitored daily and weighed once a week. The tumor volume was estimated according to the

formula of volume=L × $W^2$ × 0.52. After 3 weeks of treatment, the mice were euthanized and the tumors were dissected, weighed and fixed in 10% neutralized formalin for histological analysis as previously described (30).

*Immunohistochemistry and TUNEL assays.* Hematoxylin and eosin (H&E) and immunohistochemistry (IHC) staining were routinely performed as described previously (30). Briefly, the tumor tissue was processed into paraffin-embedded block and cut into 4 μm of thickness sections, and then applied to H&E or IHC staining of Ki67 (Novus Biologicals LLC, Littleton, CO), p53 and p21[Cip1]. Terminal deoxynucleotidyl transferase-mediated dUTP Nick End Labeling (TUNEL) assay was conducted to evaluate the apoptosis index using the FragEL™ DNA fragmentation Detection Kit (Calbiochem, La Jolla, CA), according to the users' manual.

*Statistical analyses.* ANOVA and the appropriate *post-hoc* tests were used to determine the statistical significance among multiple groups. Two-tailed *t*-test was used for comparing the tumor weight between the control and CHO27-treated groups.

## Results

*In vitro cytotoxicity screening of chalcone-based compounds.* Our previous study found that the 1-(3,4,5-trimethoxy) functional group of the chalcone greatly enhanced their cellular activity (14). A study by Ducki *et al*. demonstrated that an introduction of a 2-methyl functional group further improved chalcone's cytotoxic potency (23). In order to minimize the potential metabolism liability of the phenol functional groups, we designed and synthesized CHO27, which is a 2-methyl-1-(3,4,5-trimethoxy) functionalized chalcone without any phenol functional group (Figure 1). We first evaluated the cytotoxicity of CHO27 in comparison to the parent compound and several related chalcone-based natural products among four human cancer cell lines, representing malignancies from prostate, lung, colon and pancreas (Table I). Similar as others have reported, the plain chalcone and other chalcone-based natural products demonstrated moderate (half maximal inhibitory concentrations [$IC_{50}$] in 5-27 micromolar range) cytotoxicity
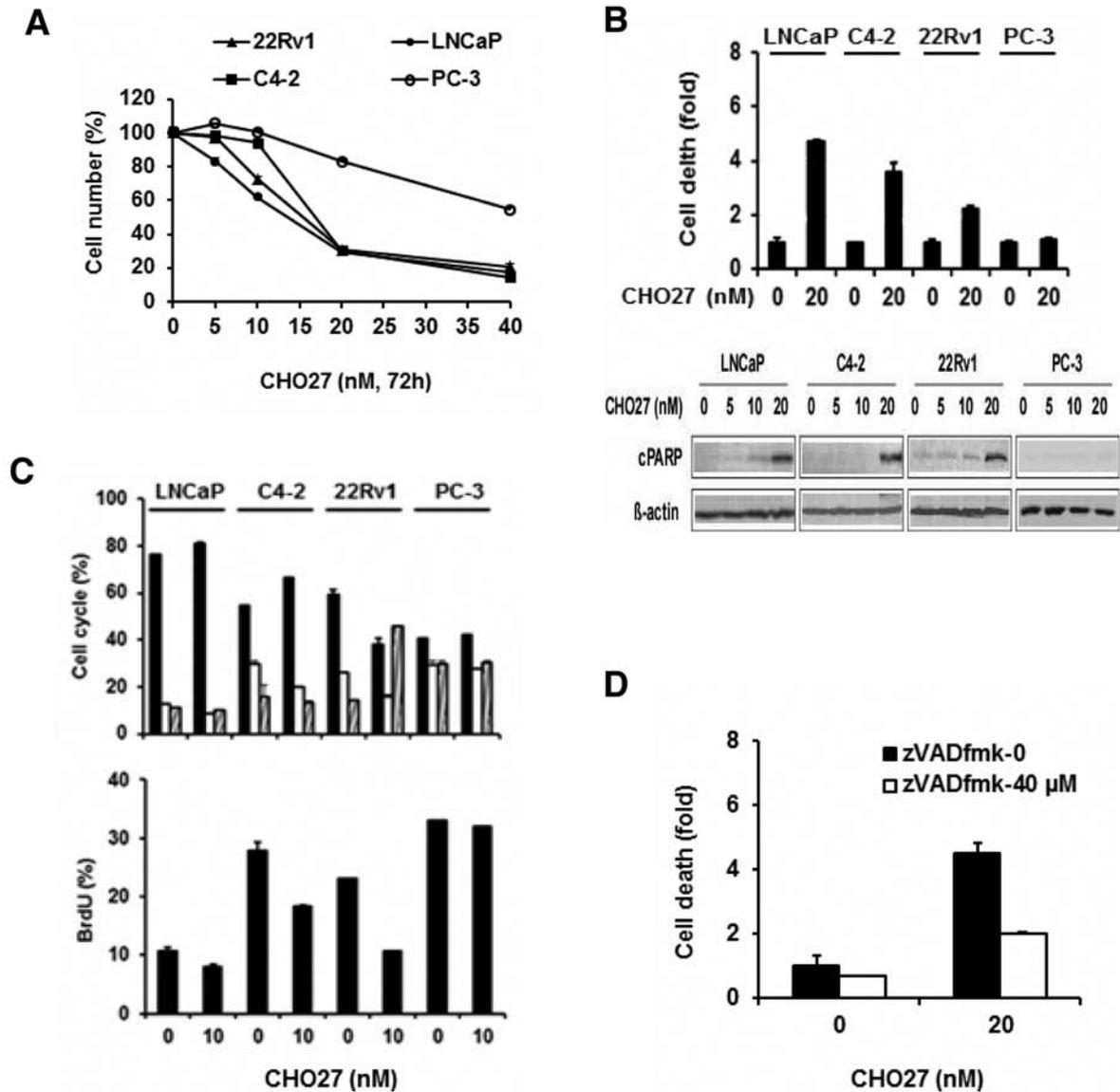
Figure 2. *Inhibitory activities of CHO27 against PCa cells in monolayer cell culture. A. Growth inhibition induced by CHO27 in PCa cells (72-h exposure) estimated by crystal violet staining of cellular protein. B. Cell death induced by CHO27 exposure in PCa cells. Upper graph: ELISA detection of apoptotic DNA nucleosomal fragmentation (72-h exposure); Lower image: immunoblotting detection of cleaved PARP (48-h exposure). C. Cell cycle distribution and BrdU incorporation rate in PCa cells exposed to CHO27 for 24 h. D. Attenuation of CHO27-induced apoptosis by a general caspase inhibitor zVADfmk (ELISA detection of apoptotic DNA nucleosomal fragmentation, 72-h exposure) in LNCaP cells. The cell growth assays were run in triplicate. Each point or column represents mean±SEM.*

against these cells. CHO27 was 175- to 1000-fold more potent than chalcone among all the cells tested. The low nanomolar range for $IC_{50}$ for CHO27 prompted further evaluation against additional PCa cells.

*CHO27 inhibited PCa cell growth with a preference for p53-wt/functional cells.* LNCaP, C4-2 and 22Rv1 and PC-3 cells were exposed to indicated concentrations of CHO27 for 72 h, and then the numbers of cells remaining adherent were estimated through crystal violet staining of cellular proteins. As shown in Figure 2A, all tested cells responded to CHO27 exposure in concentration-dependent manners with $IC_{50}$ ranging from ~13 nM to ~40 nM. The p53-wt/functional cells (LNCaP, C4-2 and 22Rv1) were more sensitive than the p53-null cells (PC-3) (Figure 2A). Similarly, the p53-wt HCT 116 and NCI-H460 cells also showed lower $IC_{50}$ than
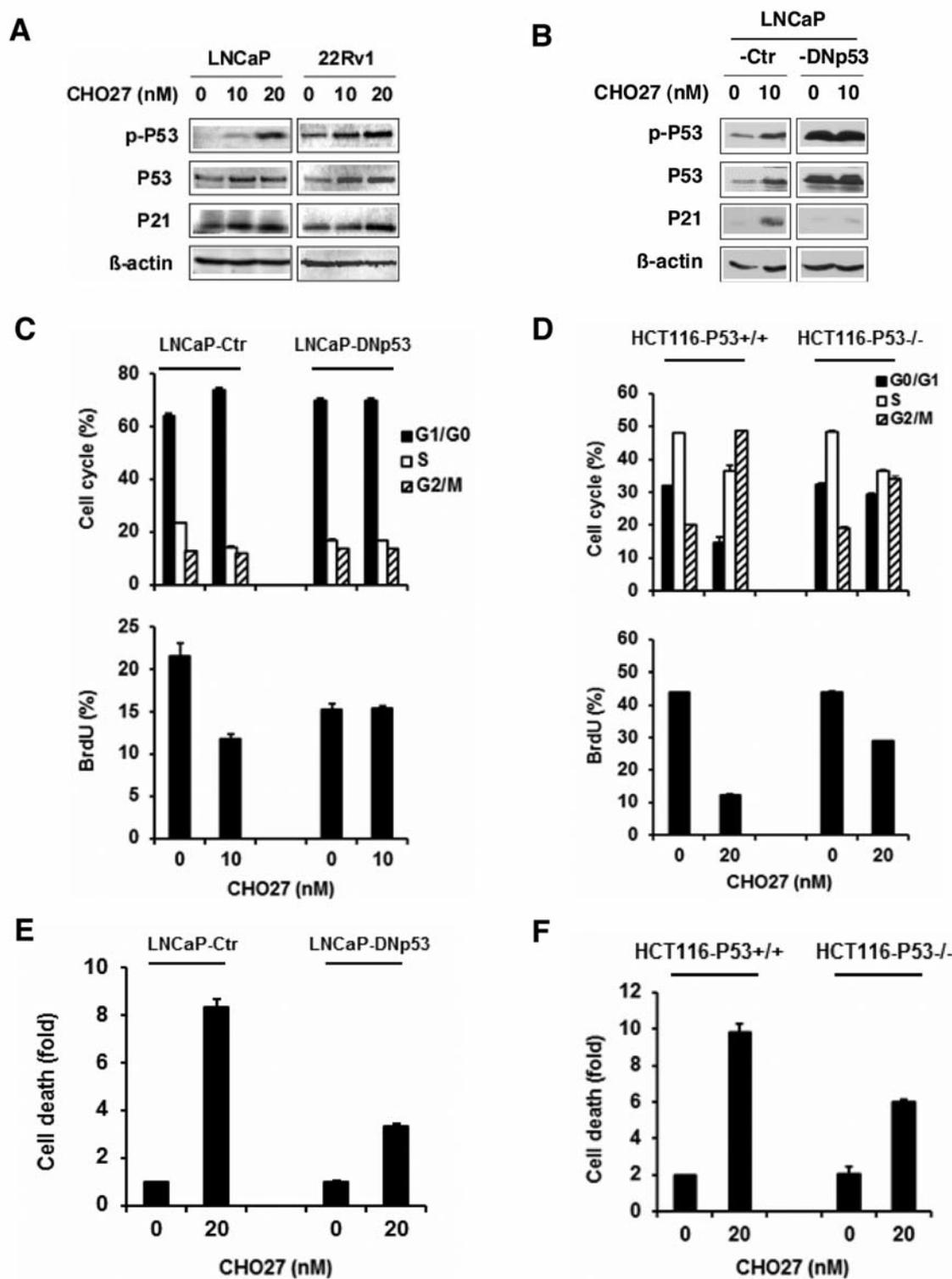
Figure 3. *Activation of p53 partially mediated the inhibitory activities of CHO27. A. Immunoblotting detection of activation of p53 in LNCaP and 22Rv1 cells (48-h exposure). B. Immunoblotting detection of the components of p53 pathway in the LNCaP-DNp53 cells and LNCaP-Ctr cells (48-h exposure). C-D. Cell cycle distribution and BrdU incorporation rate in LNCaP-Ctr and LN-DNp53 cells (C) or HCT 116-p53$^{+/+}$ and HCT 116-p53$^{-/-}$ cells (D) after 24-h exposure. E. ELISA detection of apoptotic DNA nucleosomal fragmentation in LNCaP-Ctr and DNP53-DNp53 cells after 72-h exposure. F. Annexin V staining of externalized phosphatidylserine in HCT 116-p53$^{+/+}$ and HCT 116-p53$^{-/-}$ cells after 72-h exposure. The experiments were run in triplicate. Each column represents the mean±SEM. LNCaP-Ctr and LNCaP-DNp53: LNCaP cells expressing a control or domain-negative p53 [DNp53] transfectant, respectively. HCT 116-p53$^{+/+}$ and HCT 116-p53$^{-/-}$: HCT 116 cells with wild type-p53 or deleted-p53, respectively.*
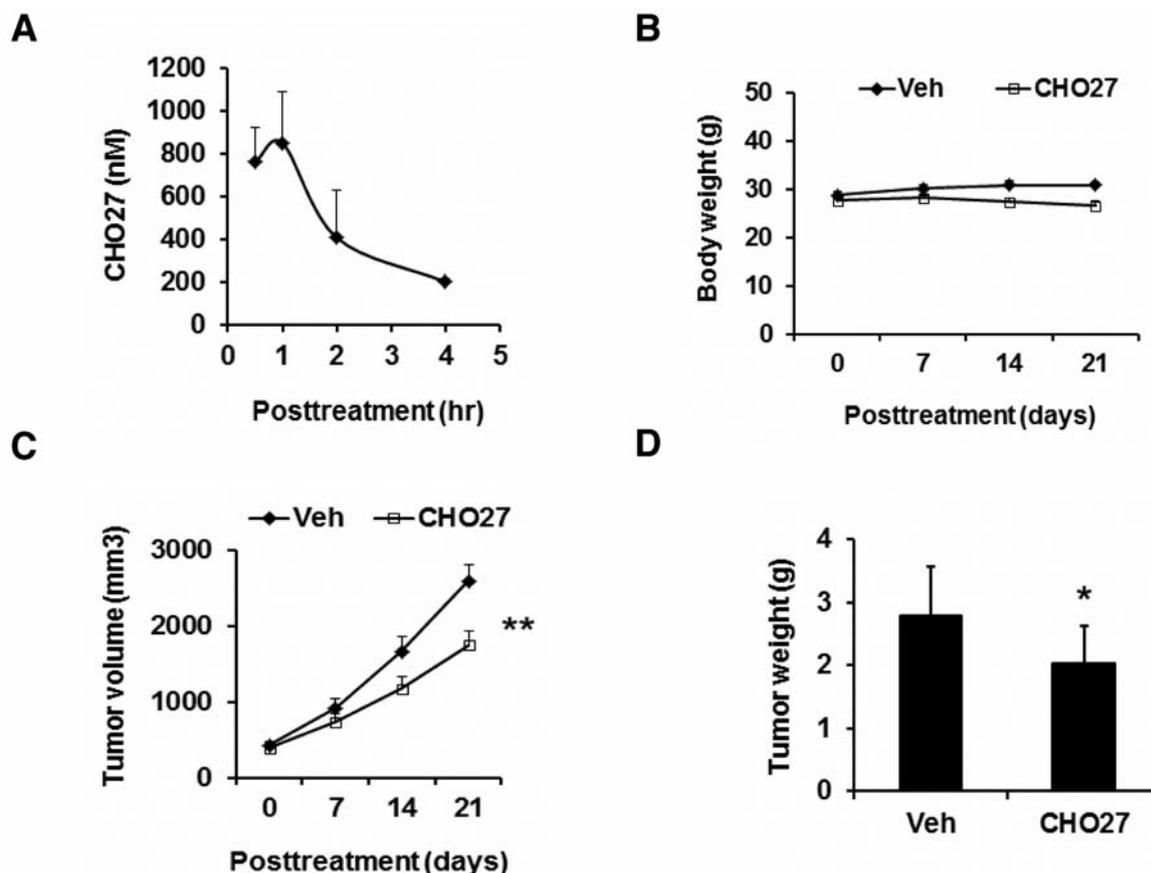
Figure 4. *Plasma pharmacokinetics of CHO27 in C75BL/6J mice and in vivo efficacy of CHO27 against 22Rv1 xenograft tumors in athymic nude mice. A. Mouse plasma concentration of CHO27 after one i.p. dose. Mean±SEM, n=3. B. Effect of CHO27 on mouse body weight. Veh and CHO27: vehicle-treated or CHO27-treated group, respectively. C. Once daily administration of CHO27 retarded 22Rv1 xenograft tumor growth. D. Final 22Rv1 xenograft tumor weights after three weeks of treatment. Each point or column represents the mean±SEM, n=11. \*: p<0.05, \*\*: p <0.01.*

the p53-mutant DU 145 and SU.86.86 cells (Table I). Taken together, the above data suggested that CHO27 at low nanomolar range inhibited PCa cells' growth with a preference for p53-wt/functional cells rather than p53-mutant/null cells.

*CHO27 induced caspase-dependent apoptosis and cell cycle arrests in PCa cells.* Pro-apoptosis is an important mechanism for therapeutic agents to eliminate malignant cells. Two independent approaches (ELISA assay of apoptotic nucleosomal fragmentation and immunoblotting detection of cleaved PARP) were used to evaluate the apoptotic action of CHO27. As shown in Figure 2B, CHO27 at 20 nM significantly increased apoptotic nucleosomal fragmentation in p53-wt/functional cells (LNCaP, C4-2 and 22Rv1), but did not do so in p53-null PC-3 cells, at 72 h of exposure. When examined after 48 h of exposure, CHO27 at 20 nM induced cleaved PARP in LNCaP, C4-2 and 22Rv1 cells, but did not do so in PC-3

cells (Figure 2B). Furthermore, a general caspase-inhibitor zVADfmk attenuated CHO27-induced apoptosis in LNCaP cells, supporting caspase-mediated death (Figure 2D).

Anti-proliferation is another mechanism for therapeutic agents to suppress tumor growth. PCa cells were exposed to sublethal concentrations of CHO27 for 24 h, and then cell cycle distribution and DNA synthesis were analyzed. As shown in Figure 2C, CHO27 at 10 nM increased $G_0/G_1$ phase cells accompanied with a reduction of S phase cells in LNCaP and C4-2 cells. CHO27 led to an accumulation of $G_2/M$ phase cells with a reduction of S phase cells in 22Rv1 cells, but did not affect PC-3 cell cycle distribution. Cellular DNA synthesis, indicated by the percentages of BrdU-incorporated cells, was decreased by CHO27 in LNCaP, C4-2 and 22Rv1 cells, but was not in PC-3 cells (Figure 2C). Taken together, the data above indicated that CHO27 could induce caspase-dependent apoptosis in many PCa cell lines and induced cell cycle arrest in $G_1$ phase or $G_2/M$ phase depending on the cell lines used.
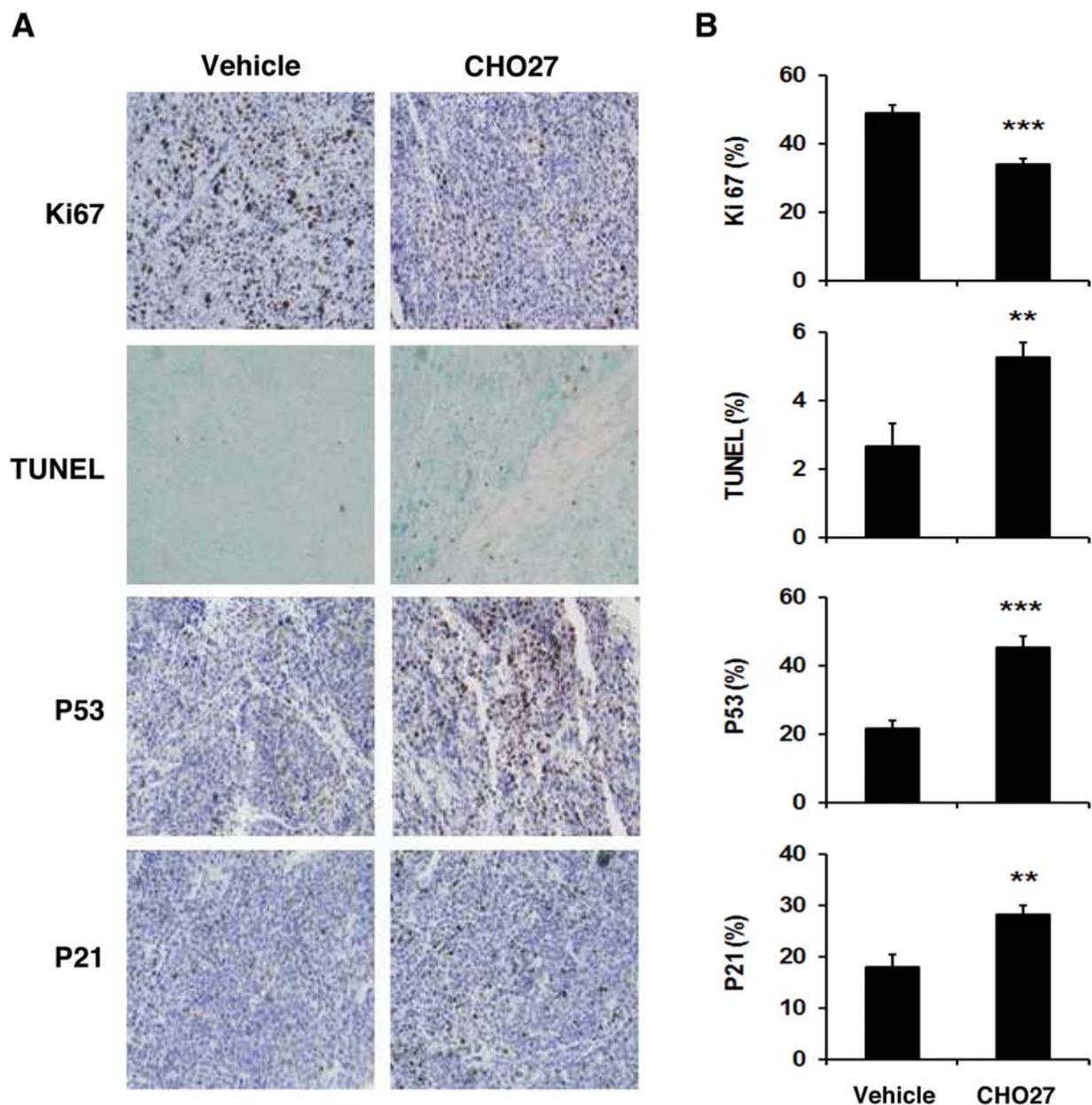
Figure 5. *Proliferation and apoptosis index and activation of p53 in 22Rv1 xenograft tumors. A. Representative images of IHC staining of Ki67, TUNEL, p53 and p21$^{Cip1}$ from each group (magnification: ×200). B. Summary of the IHC staining indexes based on 10 microscopic fields of each slide. Vehicle and CHO27: vehicle-treated or CHO27-treated group, respectively. Each column represents the mean+SEM, n=11. \*\*: p<0.01, \*\*\*: p<0.001.*

*Anti-proliferative and pro-apoptotic activity of CHO27 was associated with activation of the p53 pathway.* The differential sensitivity between p53-wt/functional *vs*. p53-mutant/null cancer cells raised a hypothesis that p53 might mediate the growth inhibitory action of CHO27. As shown in Figure 3A, CHO27 stimulated the expression and phosphorylation of p53 in LNCaP and 22Rv1 cells when examined after 48 h of exposure. p21$^{Cip1}$, a well-documented p53 downstream transcriptional target, was up-regulated accordingly. A similar observation was made for C4-2 cells (data not shown). To further delineate the role of p53 in CHO27-induced growth inhibition, we next evaluated the CHO27 effect on stable-transfectant LNCaP cells expressing a dominant-negative p53 (DNp53). As shown in Figure 3B, CHO27 up-regulated p21$^{Cip1}$ in the control cells (Ctr), but did not in the LNCaP-DNp53 cells, indicating that

the ectopic DNp53 transfectant efficiently blocked the activation of the endogenous p53 pathway. The inactivation of the p53 pathway abolished CHO27-induced $G_1$ arrest (Figure 3C) and attenuated CHO27-induced apoptosis (Figure 3E) in LNCaP cells. In addition, in *p53*-knockout colon cancer HCT 116 cells, the cell cycle arrest by CHO27 ($G_2$/M arrest) (Figure 3D) and apoptosis (Figure 3F) were significantly attenuated compared to the wild-type parental HCT 116 cells. These data supported activation of p53 signaling pathway as crucial for inducing growth inhibitory and apoptosis by CHO27 in cell culture.

*Efficacy of CHO27 against aggressive established 22Rv1 xenograft tumors in vivo.* Encouraged by the *in vitro* data, we carried out animal experiments to evaluate the pharmacokinetic parameters of CHO27 in mice and the *in vivo* inhibitory potency of CHO27 against aggressive CRPCa xenograft tumors in immunodeficient host mice. After one *i.p.* dose of administration (1 mg per mouse, ~40 mg/kg body weight), plasma CHO27 achieved a peak level of ~850 nM by 1 h, then decreased to ~400 nM by 2 h and ~200 nM by 4 h (Figure 4A). Notably, the maximum concentration (Cmax) of CHO27 in plasma was an order of magnitude higher than those required to trigger the growth inhibitory actions indicated by the above *in vitro* data.

For PCa treatment efficacy, male Nu/Nu nude mice bearing established xenografts with 22Rv1 PCa cells (~400 mm$^3$), were treated once daily by *i.p.* injection with vehicle or CHO27 (1 mg per mouse, ~40 mg/kg) for three weeks. CHO27 slightly impacted on the mouse body weights (Figure 4B). Compared to the vehicle, CHO27 treatment retarded the growth of 22Rv1 xenograft tumors (Figure 4C) and decreased the final tumor weight by 30 % ($p<0.05$) (Figure 4D). Decreased Ki67 and increased TUNEL indexes were observed in CHO27-treated tumors (Figure 5), indicating an inhibition of proliferation and induction of apoptosis in these tumors. Increased p53 and p21$^{Cip1}$ IHC staining were also observed in the CHO27-treated tumors (Figure 5). Taken together, the data indicated that CHO27 suppressed aggressive 22Rv1 tumor growth *in vivo*, accompanied by an inhibition of proliferation, induction of apoptosis and activation of the p53 signaling pathway.

## Discussion

We report here that CHO27, at low nanomolar levels (5-40 nM), exhibited inhibitory activities against various PCa cells (Figure 2A). CHO27 inhibited PCa cell growth through induction of cell cycle arrests ($G_1$ or $G_2$/M) (Figure 2C) and caspase-dependent apoptosis (Figure 2B and D). *In vivo* administration of CHO27 triggered growth inhibition of established aggressive PCa 22Rv1 xenograft tumors in a therapy context, in association with inhibition of proliferation, induction of apoptosis and activation of the p53 signaling pathway (Figure 4 and 5).

Since the majority of prostate tumors harbor wild-type p53, pharmacological activation of p53 remains a viable approach to intervene PCa (37). p53 can be rapidly activated by some oncogenes, DNA damage and therapeutic agents (38). Activation of p53 induces cell cycle checkpoint $G_1$ or $G_2$/M arrest, apoptosis, differentiation or senescence in cancer cells depending on the cell lines (38, 39). Previous studies have suggested p53 pathway activation by chalcones, for example, in colon, breast, lung and liver cancer cells (13, 27-29). The inhibitory activities of these chalcones rely on a functional activation of p53 (28, 29). Our data agreed well with these findings, *i.e.*, i) CHO27 exhibited a preferential inhibition of cell proliferation and induction of apoptosis for p53-wt/functional cancer cells than p53-mutant/null cancer cells (Table I and Figure 2A-C); ii) CHO27 activated the p53-p21$^{Cip1}$ pathway (Figure 3A); and iii) blocking of the p53 pathway abolished or attenuated CHO27-induced cell cycle arrests and apoptosis (Figure 3C-F).

p53 function is negatively-regulated by MDM2, a primary E3 ubiquitin ligase binding to p53 to form an MDM2-p53 complex leading to proteosomal degradation of p53 and inhibiting p53 transactivation activity (40-44). Disrupting the MDM2-p53 complex leads to increased p53 stability and transactivation activity of p53, which consequently restore the protective and therapeutic potential of p53. Several reports have suggested a direct action of select chalcones on the p53-MDM2 complex (45, 46). Stoll *et al.* have experimentally demonstrated that chalcones could bind competitively to the p53-binding cleft of the MDM2 (46). Our computational modeling predicted binding affinity of CHO27 to the p53 binding cleft of the MDM2 (data not shown), implying a potential direct action of CHO27 on p53-MDM2 complex. However, other indirect mechanisms through which CHO27 activates p53, such as genotoxic/ROS stress, cannot be excluded. The precise mechanisms of CHO27 activating p53 merit more investigation in the future.

Although the present study suggested p53 as a molecular target of CHO27, additional molecular targets may also be involved in the inhibitory actions of CHO27, in that blocking of the p53 pathway did not completely restore the proliferation and survival of the cells exposed to CHO27 (Figure 3C-F) and the growth of p53-null PC-3 cells was suppressed by CHO27, albeit at higher levels than required for the p53 wt/functional cells. Consistent with this hypothesis, several reports have suggested the NF-κB pathway (14, 47, 48) and Bcl-2 families (24, 49, 50) as additional molecular targets of chalcones.

In summary, the present study showed that CHO27 exerted strong cytotoxicity against PCa cells *in vitro*, in part through activating the p53-signaling pathway. The *in vivo* efficacy of CHO27 against an aggressive model of PCa in a chemotherapy context suggested its potential as a prototype lead compound for development of new therapeutic agents for PCa.

## Conflicts of Interest

## Funding Support

## Acknowledgements

## References

1 Jemal A, Siegel R, Xu J and Ward E: Cancer statistics, 2010. CA Cancer J Clin *60*: 277-300, 2010.

2 Mottet N, Bellmunt J, Bolla M, Joniau S, Mason M, Matveev V, Schmid HP, van der Kwast T, Wiegel T, Zattoni F and Heidenreich A: EAU Guidelines on Prostate Cancer. Part II: Treatment of Advanced, Relapsing, and Castration-Resistant Prostate Cancer. Actas Urologicas Espanolas *35*: 565-579, 2011.

3 de Bono JS, Logothetis CJ, Molina A, Fizazi K, North S, Chu L, Chi KN, Jones RJ, Goodman OB Jr., Saad F, Staffurth JN, Mainwaring P, Harland S, Flaig TW, Hutson TE, Cheng T, Patterson H, Hainsworth JD, Ryan CJ, Sternberg CN, Ellard SL, Flechon A, Saleh M, Scholz M, Efstathiou E, Zivi A, Bianchini D, Loriot Y, Chieffo N, Kheoh T, Haqq CM and Scher HI: Abiraterone and increased survival in metastatic prostate cancer. New Engl J Med *364*: 1995-2005, 2011.

4 Walsh PC: Re: Abiraterone and increased survival in metastatic prostate cancer. J Urol *186*: 2253-2254, 2011.

5 Dharmaratne HR, Nanayakkara NP and Khan IA: Kavalactones from Piper methysticum, and their 13C NMR spectroscopic analyses. Phytochemistry *59*: 429-433, 2002.

6 Tang Y, Li X, Liu Z, Simoneau AR, Xie J and Zi X: Flavokawain B, a kava chalcone, induces apoptosis *via* up-regulation of death-receptor 5 and Bim expression in androgen receptor negative, hormonal refractory prostate cancer cell lines and reduces tumor growth. International journal of cancer. Int J Cancer *127*: 1758-1768, 2010.

7 Szliszka E, Czuba ZP, Mazur B, Paradysz A and Krol W: Chalcones and dihydrochalcones augment TRAIL-mediated apoptosis in prostate cancer cells. Molecules *15*: 5336-5353, 2010.

8 Kanazawa M, Satomi Y, Mizutani Y, Ukimura O, Kawauchi A, Sakai T, Baba M, Okuyama T, Nishino H and Miki T: Isoliquiritigenin inhibits the growth of prostate cancer. Europ Urology *43*: 580-586, 2003.

9 Yamazaki S, Morita T, Endo H, Hamamoto T, Baba M, Joichi Y, Kaneko S, Okada Y, Okuyama T, Nishino H and Tokue A: Isoliquiritigenin suppresses pulmonary metastasis of mouse renal cell carcinoma. Cancer Lett *183*: 23-30, 2002.

10 Kim do Y, Kim KH, Kim ND, Lee KY, Han CK, Yoon JH, Moon SK, Lee SS and Seong BL: Design and biological evaluation of novel tubulin inhibitors as antimitotic agents using a pharmacophore binding model with tubulin. J Medicinal Chem *49*: 5664-5670, 2006.

11 Baba M, Asano R, Takigami I, Takahashi T, Ohmura M, Okada Y, Sugimoto H, Arika T, Nishino H and Okuyama T: Studies on cancer chemoprevention by traditional folk medicines XXV. Inhibitory effect of isoliquiritigenin on azoxymethane-induced murine colon aberrant crypt focus formation and carcinogenesis. Biol Pharm Bull *25*: 247-250, 2002.

12 Takahashi T, Takasuka N, Iigo M, Baba M, Nishino H, Tsuda H and Okuyama T: Isoliquiritigenin, a flavonoid from licorice, reduces prostaglandin E2 and nitric oxide, causes apoptosis, and suppresses aberrant crypt foci development. Cancer Science *95*: 448-453, 2004.

13 Achanta G, Modzelewska A, Feng L, Khan SR and Huang P: A boronic-chalcone derivative exhibits potent anticancer activity through inhibition of the proteasome. Molecular Pharmacol *70*: 426-433, 2006.

14 Srinivasan B, Johnson TE, Lad R and Xing C: Structure-activity relationship studies of chalcone leading to 3-hydroxy-4,3',4',5'-tetramethoxychalcone and its analogues as potent nuclear factor kappaB inhibitors and their anticancer activities. J Medicinal Chem *52*: 7228-7235, 2009.

15 Srinivasan B, Johnson TE and Xing C: Chalcone-based inhibitors against hypoxia-inducible factor 1 – structure activity relationship studies. Bioorganic Medicinal Chem Lett *21*: 555-557, 2011.

16 Wattenberg LW, Coccia JB and Galbraith AR: Inhibition of carcinogen-induced pulmonary and mammary carcinogenesis by chalcone administered subsequent to carcinogen exposure. Cancer Lett *83*: 165-169, 1994.

17 Wattenberg L: Chalcones, myo-inositol and other novel inhibitors of pulmonary carcinogenesis. J Cell Biochem *22*: 162-168, 1995.

18 Hsu YL, Kuo PL, Chiang LC and Lin CC: Isoliquiritigenin inhibits the proliferation and induces the apoptosis of human non-small cell lung cancer a549 cells. Clin Exp Pharmacol Physiol *31*: 414-418, 2004.

19 Lee SH, Zhao YZ, Park EJ, Che XH, Seo GS and Sohn DH: 2',4',6'-Tris(methoxymethoxy) chalcone induces apoptosis by enhancing Fas-ligand in activated hepatic stellate cells. Eur J Pharmacol *658*: 9-15, 2011.

20 Ye CL, Liu JW, Wei DZ, Lu YH and Qian F: *In vivo* antitumor activity by 2',4'-dihydroxy-6'-methoxy-3',5'-dimethylchalcone in a solid human carcinoma xenograft model. Cancer Chem Pharmacol *56*: 70-74, 2005.

21 Tang Y, Simoneau AR, Xie J, Shahandeh B and Zi X: Effects of the kava chalcone flavokawain A differ in bladder cancer cells with wild-type *versus* mutant p53. Cancer Prev Res *1*: 439-451, 2008.

22 Zi X and Simoneau AR: Flavokawain A, a novel chalcone from kava extract, induces apoptosis in bladder cancer cells by involvement of Bax protein-dependent and mitochondria-dependent apoptotic pathway and suppresses tumor growth in mice. Cancer Res *65*: 3479-3486, 2005.

23 Ducki S, Forrest R, Hadfield JA, Kendall A, Lawrence NJ, McGown AT and Rennison D: Potent antimitotic and cell growth inhibitory properties of substituted chalcones. Bioorganic Medicinal Chem Lett *8*: 1051-1056, 1998.

24 Lin E, Lin WH, Wang SY, Chen CS, Liao JW, Chang HW, Chen SC, Lin KY, Wang L, Yang HL and Hseu YC: Flavokawain B inhibits growth of human squamous carcinoma cells: Involvement of apoptosis and cell cycle dysregulation *in vitro* and *in vivo*. J Nutritional Biochem *23*: 368-378, 2011.

25 Go ML, Wu X and Liu XL: Chalcones: an update on cytotoxic and chemoprotective properties. Current Medicinal Chem *12*: 481-499, 2005.

26 Boumendjel A, Ronot X and Boutonnat J: Chalcones derivatives acting as cell cycle blockers: potential anti cancer drugs? Current Drug Targets *10*: 363-371, 2009.

27 Modzelewska A, Pettit C, Achanta G, Davidson NE, Huang P and Khan SR: Anticancer activities of novel chalcone and bis-chalcone derivatives. Bioorganic Medicinal Chem Lett *14*: 3491-3495, 2006.

28 Rao YK, Kao TY, Ko JL and Tzeng YM: Chalcone HTMC causes *in vitro* selective cytotoxicity, cell-cycle G1 phase arrest through p53-dependent pathway in human lung adenocarcinoma A549 cells, and *in vivo* tumor growth suppression. Bioorganic Medicinal Chem Lett *20*: 6508-6512, 2010.

29 HSU YL, Kuo PO and Lin CC: Isoliquiritigenin induces apoptosis and cell cycle arrest through p53-dependent pathway in Hep G2 cells. Life Sci *77*: 279-292, 2004.

30 Zhang Y, Zhang J, Wang L, Quealy E, Gary BD, Reynolds RC, Piazza GA and Lu J: A novel sulindac derivative lacking cyclooxygenase-inhibitory activities suppresses carcinogenesis in the transgenic adenocarcinoma of mouse prostate model. Cancer Prev Res (Phila) *3*: 885-895, 2010.

31 Malewicz B, Wang Z, Jiang C, Guo J, Cleary MP, Grande JP and Lu J: Enhancement of mammary carcinogenesis in two rodent models by silymarin dietary supplements. Carcinogenesis *27*: 1739-1747, 2006.

32 Jiang C, Wang Z, Ganther H and Lu J: Caspases as key executors of methyl selenium-induced apoptosis (anoikis) of DU-145 prostate cancer cells. Cancer Res *61*: 3062-3070, 2001.

33 Hu H, Jiang C, Ip C, Rustum YM and Lu J: Methylseleninic acid potentiates apoptosis induced by chemotherapeutic drugs in androgen-independent prostate cancer cells. Clin Cancer Res *11*: 2379-2388, 2005.

34 Hu H, Jiang C, Schuster T, Li GX, Daniel PT and Lu J: Inorganic selenium sensitizes prostate cancer cells to TRAIL-induced apoptosis through superoxide/p53/Bax-mediated activation of mitochondrial pathway. Mol Cancer Ther *5*: 1873-1882, 2006.

35 Zhang Y, Kim KH, Zhang W, Guo Y, Kim SH and Lu J: Galbanic acid decreases androgen receptor abundance and signaling and induces G(1) arrest in prostate cancer cells. Int J Cancer *130*: 200-212, 2011.

36 Li L, Shaik AA, Zhang J, Nhkata K, Wang L, Zhang Y, Xing C, Kim SH and Lu J: Preparation of penta-O-galloyl-beta-D-glucose from tannic acid and plasma pharmacokinetic analyses by liquid-liquid extraction and reverse-phase HPLC. J Pharm Biomed Anal *54*: 545-550, 2011.

37 Tovar C, Higgins B, Kolinsky K, Xia M, Packman K, Heimbrook DC and Vassilev LT: MDM2 antagonists boost antitumor effect of androgen withdrawal: implications for therapy of prostate cancer. Molecular cancer *10*: 49-60, 2011.

38 Jin S and Levine AJ: The p53 functional circuit. J Cell Science *114*: 4139-4140, 2001.

39 Agarwal ML, Agarwal A, Taylor WR and Stark GR: p53 controls both the $G_2/M$ and the $G_1$ cell cycle checkpoints and mediates reversible growth arrest in human fibroblasts. Proc Nat Acad Sci USA *92*: 8493-8497, 1995.

40 Wu X, Bayle JH, Olson D and Levine AJ: The p53-mdm-2 autoregulatory feedback loop. Genes Develop *7*: 1126-1132, 1993.

41 Bond GL, Hu W and Levine AJ: MDM2 is a central node in the p53 pathway: 12 years and counting. Current Cancer Drug Targets *5*: 3-8, 2005.

42 Kubbutat MH, Jones SN and Vousden KH: Regulation of p53 stability by Mdm2. Nature *387*: 299-303, 1997.

43 Haupt Y, Maya R, Kazaz A and Oren M: Mdm2 promotes the rapid degradation of p53. Nature *387*: 296-299, 1997.

44 Rayburn ER, Ezell SJ and Zhang R: Recent advances in validating MDM2 as a cancer target. Anti-cancer Agents Medicinal Chem *9*: 882-903, 2009.

45 Chen Z, Knutson E, Wang S, Martinez LA and Albrecht T: Stabilization of p53 in human cytomegalovirus-initiated cells is associated with sequestration of HDM2 and decreased p53 ubiquitination. J Biol Chem *282*: 29284-29295, 2007.

46 Stoll R, Renner C, Hansen S, Palme S, Klein C, Belling A, Zeslawski W, Kamionka M, Rehm T, Muhlhahn P, Schumacher R, Hesse F, Kaluza B, Voelter W, Engh RA and Holak TA: Chalcone derivatives antagonize interactions between the human oncoprotein MDM2 and p53. Biochemistry *40*: 336-344, 2001.

47 Kamal A, Dastagiri D, Ramaiah MJ, Reddy JS, Bharathi EV, Srinivas C, Pushpavalli SN, Pal D and Pal-Bhadra M: Synthesis of imidazothiazole-chalcone derivatives as anticancer and apoptosis inducing agents. ChemMedChem *5*: 1937-1947, 2010.

48 Liu YC, Hsieh CW, Wu CC and Wung BS: Chalcone inhibits the activation of NF-kappaB and STAT3 in endothelial cells *via* endogenous electrophile. Life Sci *80*: 1420-1430, 2007.

49 Fang SC, Hsu CL, Yu YS and Yen GC: Cytotoxic effects of new geranyl chalcone derivatives isolated from the leaves of Artocarpus communis in SW 872 human liposarcoma cells. J Agricultural Food Chem *56*: 8859-8868, 2008.

50 Hsu YL, Kuo PL, Tzeng WS and Lin CC: Chalcone inhibits the proliferation of human breast cancer cell by blocking cell cycle progression and inducing apoptosis. Food Chemical Toxicol *44*: 704-713, 2006.